Cellular uptake of *N*-acetyl-D-galactosamine-, *N*-acetyl-D-glucosamine- and D-mannose-containing fluorescent glycoconjugates investigated by liver intravital microscopy

Svetlana Yu. Maklakova[a,*], Victor A. Naumenko[b,1], Andrey D. Chuprov[a], Maria P. Mazhuga[a], Nikolai V. Zyk[a], Elena K. Beloglazkina[a], Alexander G. Majouga[a,b,c]

[a] *Department of Chemistry, Lomonosov Moscow State University, Leninskie Gory, 1/3, 119991, Moscow, Russia*
[b] *National University of Science and Technology MISiS, Leninsky Ave, 4, 119049, Moscow, Russia*
[c] *D. I. Mendeleev University of Chemical Technology of Russia, Miusskaya sq., 9, 125047, Moscow, Russia*

1. Introduction

The object of targeted drug delivery is to provide specific localization of a drug in the site of action in therapeutically acceptable dose. As a result, it could be a way to improve bioavailability and biodistribution profile of a therapeutic agent and the efficacy and safety of the whole treatment [1]. Speaking about targeted drug delivery one can't but mention conjugates of oligonucleotides (ONs) and synthetic multivalent ligands of the asialoglycoprotein receptor (ASGPR) that are claimed to be the most successful oligonucleotide delivery system to date [2]. The ligands effectively bind to ASGPR that is highly expressed on hepatocytes resulting in rapid endocytosis of the conjugate. Unlike alternative ONs delivery systems based on nanoparticles, conjugates are simpler, smaller, and compositionally defined. By the year 2018, clinical trials of ONs conjugates, including phase III trials, were underway by at least three companies to treat a wide variety of diseases [2,3]. This success arouses great interest in novel molecules capable of binding to the receptor and thorough study of newly designed compounds as well as known ones.

The efficiency of receptor−ligand interaction and the ligand's influence on the uptake of the conjugate are commonly studied *in vitro* or *ex vivo*. Here we report the results obtained by intravital microscopy that allowed us to trace in real time internalization and accumulation of three fluorescent glycoconjugates in liver cells. To the best of our knowledge, intravital microscopy has never been used to investigate biological properties of ASGPR ligands.

ASGPR is known to facilitate uptake and clearance of glycoproteins, containing terminal D-galactose and *N*-acetyl-D-galactosamine (GalNAc) residues [4]. It is also established, that in contrast to monovalent, multivalent ligands (containing three or four terminal carbohydrate moieties) show dramatically enhanced binding affinity towards the receptor [5]. In this work to obtain a fluorescent glycoconjugate we chose a scaffold with three GalNAc residues that was identified during the comprehensive investigation of structure−activity relationships of ASGPR multivalent ligands [6].

We also studied *N*-acetyl-D-glucosamine (GlcNAc) and D-mannose (Man) based compounds structurally close to the ligand under investigation to compare the obtained results. According to the literature data, ASGPR does not interact with derivatives of these carbohydrates.

2. Results and discussion

2.1. Synthesis of the conjugates

Previously reported triantennary GalNAc ligand [6] was slightly reengineered to facilitate covalent conjugation to commercially available fluorescent dye *sulfo*-Cy5 alkyne. Namely, it was functionalized with a terminal azido group to make it applicable for Cu(I)-catalyzed azide-alkyne cycloaddition (CuAAC) (Fig. 1).

Synthetic protocol for the preparation of GalNAc ligand **1a** was described in our previous work [7] and in this study it was successfully applied to obtain GlcNAc- and Man-containing compounds **1b** and **1c** (Scheme 1). Two building blocks (active ester of tricarboxylic acid **2** and carbohydrate-containing amines **3b** and **3c**) were put into reaction to furnish the intermediates **4b** and **4c** bearing protecting acetyl groups. Compounds **4b** and **4c** were subjected to alkali alcoholysis to yield unprotected triglycosylated azides **1b** and **1c**.

The building blocks were obtained from commercially available reagents. Triacid **2** comprising azido group was readily synthesized in 3 steps from TRIS, *tert*-butyl acrylate and 11-azidoundecanoic acid as described [8]. The acid was converted to the active ester by reacting with *N*-hydroxysuccinimide (HOSu) in the presence of *N*-(3-dimethylaminopropyl)-*N*′-ethylcarbodiimide hydrochloride (EDC). In previous works [9–11], amines **3b** and **3c** were reported to be prepared by
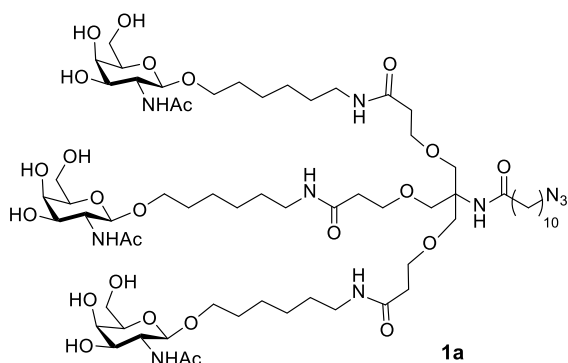
Fig. 1. Structure of the ASGPR ligand with a terminal azido group.

reduction of corresponding azides. In our case, compounds **3b** and **3c** were synthesized by glycosylation of Cbz-protected 6-amino-1-hexanol and subsequent hydrogenolysis.

The conjugates of ligands **1a-1c** with water-soluble fluorescent dye *sulfo*-Cy5 alkyne were obtained *via* CuAAC. The reaction was carried out in DMF-water solution with sodium ascorbate and copper sulfate (Scheme 2).

LCMS showed full conversion of **1a** to **5a** and pure GalNAc-containing conjugate **5a** was obtained after simple work up of the reaction mixture while compounds **5b** and **5c** were further purified by HPLC to get rid of the starting materials. As a result, the desired glycoconjugates were synthesized with good yields.

2.2. Liver intravital imaging

Using intravital microscopy we tracked in real time the microdistribution of the glycoconjugates **5a-5c** after i.v. injection.

Supplementary video related to this article can be found at https://doi.org/10.1016/j.carres.2020.107928

Immediately after i.v. injection of conjugate **5a**, the hepatic sinusoids were counterstained by Cy5. The vascular concentration of compound **5a** gradually decreased, while its accumulation in parenchymal cells increased (Fig. 2; Supplementary Video 1). During the experiment fluorescence of *sulfo*-Cy5 was clearly observed in hepatocytes, both on the cellular membrane and in the cytoplasmic vesicles, presumably in the endosomes (Fig. 3A). To show specific penetration of conjugate **5a** into hepatocytes, liver macrophages and neutrophils were stained with fluorescent antibodies (anti-F4/80-Alexa-488 and anti-Ly6G-BV421). The results indicate that conjugate **5a** does not enter macrophages and neutrophils (Fig. 3A).

Conjugates **5b** and **5c** (based on *N*-acetyl-D-glucosamine and D-mannose, respectively) were also studied using intravital microscopy (Supplementary Videos 2-3 and Fig. 3B and C). It is known [12], that mannosylated compounds as well as GlcNAc-containing compounds could be captured by carbohydrate receptors that are expressed by Kupffer cells and sinusoidal endothelial cells. In our case, conjugates **5b** and **5c** accumulated on the surface of the endothelial cells lining the hepatic sinusoids and did not demonstrate the ability to enter hepatocytes or liver macrophages.

Supplementary video related to this article can be found at https://doi.org/10.1016/j.carres.2020.107928

3. Conclusion

With the help of intravital microscopy for the first time cellular uptake of three fluorescent glycoconjugates based on *N*-acetyl-D-galactosamine, *N*-acetyl-D-glucosamine and D-mannose was traced in real time. GalNAc ligand **1a** was shown to facilitate rapid and effective penetration of the fluorophore into hepatocytes, its accumulation, and retention. On the contrast, GlcNAc- and Man-containing fluorescent

glycoconjugates did not enter parenchymal liver cells and accumulated in liver sinusoidal endothelial cells.

4. Experimental

4.1. General information

NMR spectra were recorded using Bruker Avance 400 and Agilent 400 MR instruments, and chemical shifts are reported as ppm referenced to solvent signals. High resolution mass spectra were obtained on Orbitrap Elite mass spectrometer (Thermo Fischer Scientific). For purification and analysis of samples was used a Shimadzu Prominence LC-20 system with a Phenomenex Luna 3 μm C18 90A (150 × 4.6 mm) in a column oven at 40 °C and a fraction collector coupled to single quadrupole mass spectrometer Shimadzu LCMS-2020 with a dual DUIS-ESI-APCI ionization source. Absorption spectra were taken on a Hitachi U-2900 spectrophotometer. Reagents received from commercial sources ("Sigma-Aldrich", "Carbosynth", "Lumiprobe") were used without further purification. Ligand **1a** was synthetized as described [7].

4.2. Synthesis of fluorescent glycoconjugates

4.2.1. Synthesis of compounds 3b and 3c
4.2.1.1. General procedure. The appropriate glycosyl donor (1.2 eq), benzyl *N*-(6-hydroxyhexyl)carbamate (1.0 eq) and molecular sieves (4 Å) were suspended in 1,2-dichloroethane. The suspension was stirred for half an hour before TMSOTf (0.5 eq) was added. The resulting mixture was stirred overnight. After that, it was diluted with CH_2Cl_2 and washed successively with saturated solution of $NaHCO_3$ and brine. The organic layer was dried over Na_2SO_4, and the solvent was removed under reduced pressure. Purification using silica gel column chromatography (CH_2Cl_2/MeOH, 20/1, v/v) furnished the Cbz-protected amine. To remove the protecting group it was dissolved in methanol, Pd/C (10 wt %) was added, and the resulting mixture was stirred under H_2 atmosphere overnight. The mixture was filtered over a path of Celite, and the solvent was removed under reduced pressure.

4.2.1.2. 6-Aminohexyl 2-acetamido-3,4,6-tri-O-acetyl-2-deoxy-β-D-glucopyranoside (3b). 2-Methyl-3,4,6-tri-*O*-acetyl-1,2-deoxy-α-D-glucopyrano[2,1,*d*]-2-oxazoline [13] (0.50 g, 1.5 mmol) gave **3b** (0.35 g, 63%, 2 steps) as white solid: ^{1}H NMR (DMSO-d_6, 400 MHz): δ 7.98 (d, J = 9.3 Hz, 1H, NHAc), 7.58 (br s., 2H, NH₂), 5.07 (t, J = 9.9 Hz, 1H, H-4), 4.81 (t, J = 9.9 Hz, 1H, H-3), 4.58 (d, J = 8.4 Hz, 1H, H-1), 4.17 (dd, J = 12.0, 4.0 Hz, 1H, H-6), 4.06–3.93 (m, 1H, H-6′), 3.84–3.76 (m, 1H, H-5), 3.74–3.63 (m, 2H, H-2, OCH'H''), 3.47–3.36 (m, 1H, OCH'H''), 2.73 (t, J = 7.6 Hz, 2H, CH₂NH₂), 2.02, 1.97, 1.91, 1.76 (all s, 3H each, C(O)CH₃), 1.53–1.40 (m, 4H, Aliphatics). 1.30–1.19 (m, 4H, Aliphatics).

4.2.1.3. 6-Aminohexyl 2,3,4,6-tetra-O-acetyl-α-D-mannopyranoside (3c). 2,3,4,6-tetra-*O*-acetyl-α-D-mannopyranosyl trichloroimidate [14] (3.9 g, 7.8 mmol) gave **3c** (0.9 g, 30%, 2 steps) as white solid: ^{1}H NMR (DMSO-d_6, 400 MHz): 7.86 (br s, 3H, NH₃⁺), 5.12–5.06 (m, 3H, H-2, H-3, H-4), 4.87 (br s, 1H, H-1), 4.15 (dd, J = 12.2, 5.3 Hz, 1H, H-6), 4.15 (dd, J = 12.1, 2.5 Hz, 1H, H-6′), 3.94–3.88 (m, 1H, H-5), 3.63 (dt, J = 9.7, 6.7 Hz, 1H, OCH'H''), 3.46 (dt, J = 9.7, 6.4 Hz, 1H, OCH'H''), 2.78–2.71 (m, 2H, CH₂NH₃⁺), 2.11 (s, 3H, C(O)CH₃), 2.02 (s, 6H, 2 × C(O)CH₃), 1.94 (s, 3H, C(O)CH₃), 1.61–1.50 (m, 4H, Aliphatics), 1.36–1.27 (m, 4H, Aliphatics).

4.2.2. Synthesis of compounds 4b and 4c
4.2.2.1. General procedure. 11-azido-*N*-tris-[(2-carboxyethoxy)methyl] methylundecanamide **(2)** [8] (0.22 g, 0.4 mmol) was dissolved in 5 ml of anhydrous DMF. EDC hydrochloride (0.31 g, 1.6 mmol) and NHS (0.16 g, 1.4 mmol) were added. The resulting mixture was stirred at room temperature overnight. After that, it was poured into saturated
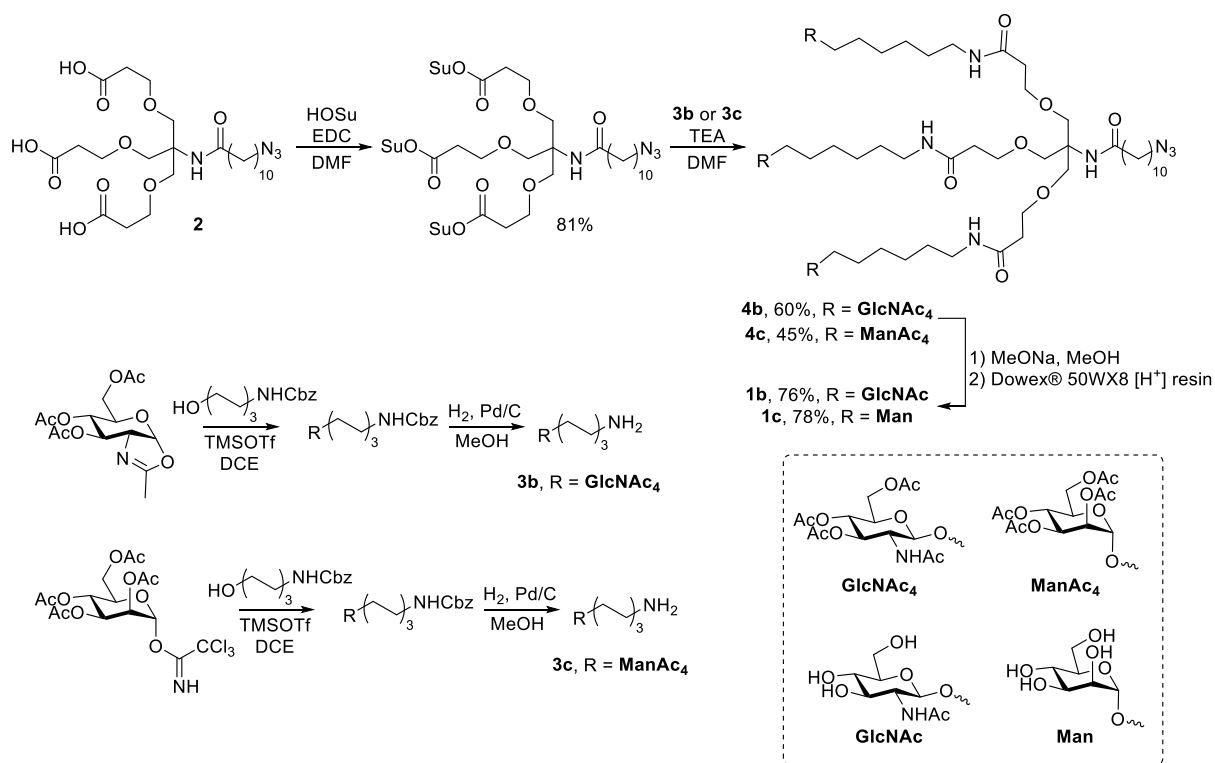
Scheme 1. Synthesis of GlcNAc- and Man-containing compounds **1b** and **1c**.
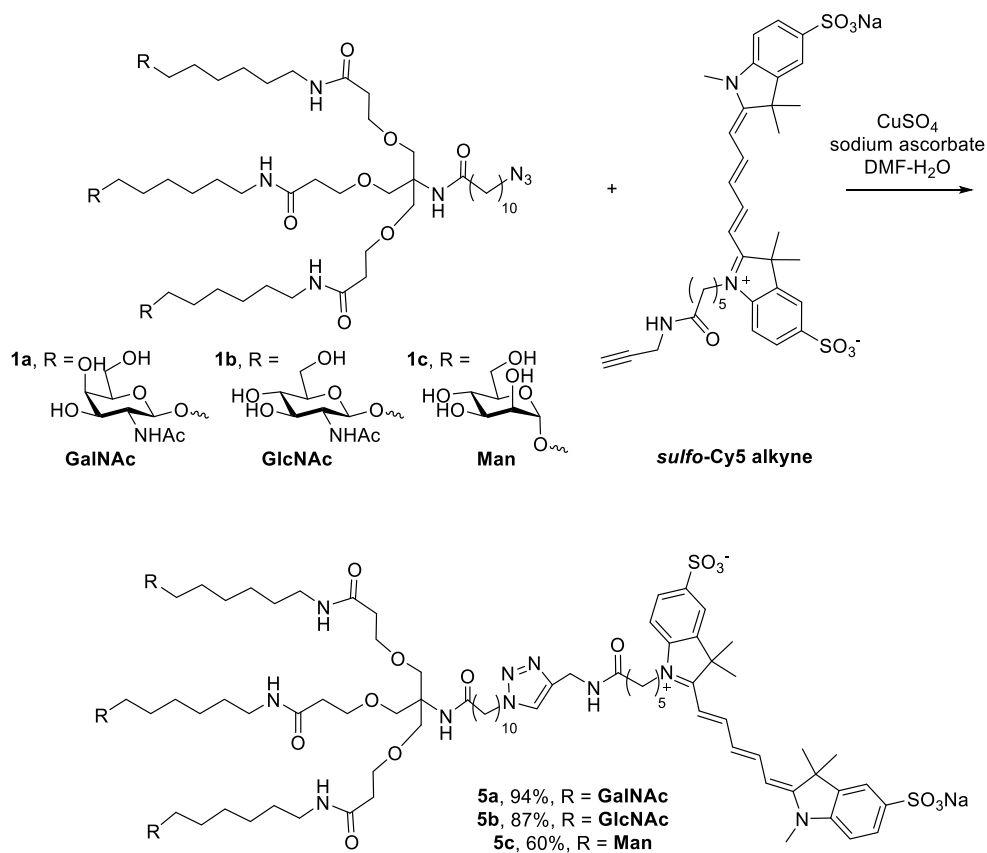
Scheme 2. Synthesis of conjugates **5a-5c**.
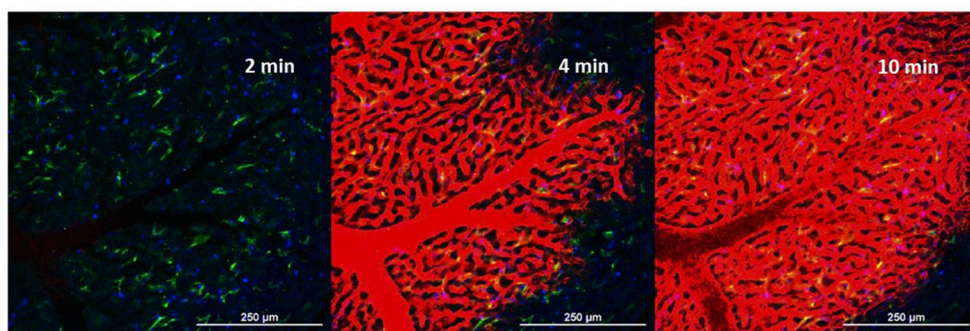
Fig. 2. Conjugate **5a** real time accumulation in liver cells: red, *sulfo*-Cy5-conjugate; blue, neutrophils; green, macrophages. Images captured 2, 4 and 10 min after i.v. injection of conjugate **5a** (see Supplementary Video 1). (For interpretation of the references to color in this figure legend, the reader is referred to the Web version of this article.)
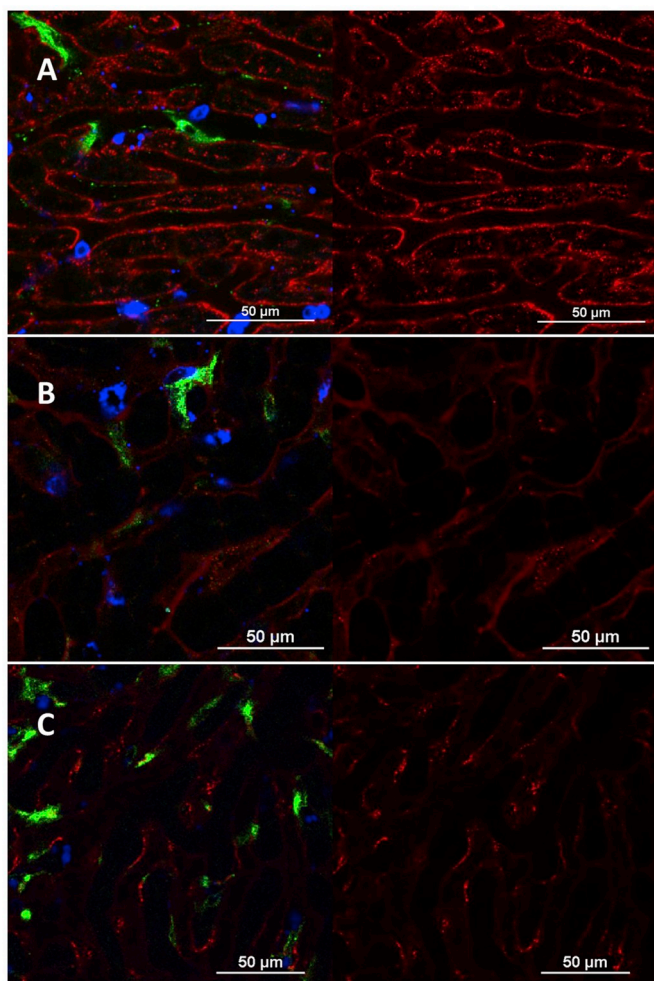
Fig. 3. Representative confocal images of liver after i.v. injection of conjugate **5a** (A), conjugate **5b** (B) and conjugate **5c** (C): red, *sulfo*-Cy5-conjugate; blue, neutrophils; green, macrophages. Macrophages and neutrophils were stained by fluorescently tagged antibodies (F4/80 Alexa 488 and Ly6G BV421, respectively). (For interpretation of the references to color in this figure legend, the reader is referred to the Web version of this article.)

solution of NaHCO$_3$, and the product was extracted with CH$_2$Cl$_2$. The organic layer was washed with brine, dried over Na$_2$SO$_4$, and the solvent was removed under reduced pressure to yield active ester (0.27 g, 81%) as colorless oil. ^{1}H NMR (CDCl$_3$, 400 MHz): δ 5.90 (br s, 1H, NH), 3.75–3.72 (m, 12H, 3 × CC$\underline{H}_2$OC$\underline{H}_2$), 3.20 (t, J = 7.0 Hz, 2H, N$_3$C$\underline{H}_2$), 2.87–2.78 (m, 18H, 3 × OCH$_2$C$\underline{H}_2$C(O), 3 × C(O)C$\underline{H}_2$C$\underline{H}_2$C(O)), 2.07 (t, J = 7.5 Hz, 2H, C$\underline{H}_2$C(O)NH), 1.57–1.50 (m, 4H, Aliphatics), 1.32–1.19 (m, 12H, Aliphatics).

To a stirred solution of NHS ester thus obtained (1 eq) and TEA (8 eq) in DMF (5 mL) was added the appropriate amine **3b** or **3c** (4 eq). The mixture was stirred at room temperature overnight. The solvent was removed under reduced pressure. The residue was suspended in EtOAc and washed successively with 1 M HCl and brine. The organic phase was dried over Na$_2$SO$_4$, filtered and concentrated under vacuum. The crude product was purified by column chromatography (CH$_2$Cl$_2$/MeOH, 50/1 → 10/1, v/v).

4.2.2.2. Compound 4b. From 100 mg (0.12 mmol) of NHS ester and 200 mg (0.45 mmol) of 6-aminohexyl 2-acetamido-3,4,6-tri-O-acetyl-2-deoxy-β-D-glucopyranoside (**3b**) there were obtained 130 mg (60%) of compound **4b** as white solid: ^{1}H NMR (CDCl$_3$, 400 MHz): δ 6.90 (br s, 1H, NH), 6.72 (d, J = 8.1 Hz, 3H, 3 × NH), 6.35 (br s, 1H, NH), 5.31 (t, J = 9.7 Hz, 3H, 3 × H-4), 5.03 (t, J = 9.7 Hz, 3H, 3 × H-3), 4.71 (d, J = 8.3 Hz, 3H, 3 × H-1), 4.25 (dd, J = 12.2, 4.7 Hz, 3H, 3 × H-6), 4.11 (dd, J = 12.2, 1.8 Hz, 3H, 3 × H-6′), 3.87–3.76 (m, 6H, 3 × H-2, 3 × H-5), 3.72–3.65 (m, 15H, 3 × OC$\underline{H}$'H", 3 × CC$\underline{H}_2$OC$\underline{H}_2$), 3.48–3.42 (m, 3H, 3 × OCH'$\underline{H}$"), 3.25–3.17 (m, 8H, 3 × (CH$_2$)$_4$C$\underline{H}_2$NH, N$_3$C$\underline{H}_2$), 2.44–2.40 (m, 6H, 3 × OCH$_2$C$\underline{H}_2$C(O)), 2.16 (t, J = 7.4 Hz, 2H, (CH$_2$)$_8$C$\underline{H}_2$C(O)), 2.06, 2.00, 2.00, 1.93 (all s, 9H each, 12 × C(O)C$\underline{H}_3$), 1.59–1.49 (m, 16H, Aliphatics), 1.33–1.26 (m, 24H, Aliphatics); ^{13}C NMR (CDCl$_3$, 100 MHz): δ 173.9, 171.5, 170.7, 170.6, 170.6, 169.4, 100.5, 72.4, 71.5, 69.5, 68.8, 67.4, 62.2, 59.4, 54.7, 51.4, 39.2, 37.1, 36.4, 29.4, 29.3, 29.3, 29.3, 29.2, 29.0, 29.0, 28.7, 26.6, 26.4, 25.7, 25.4, 23.1, 20.7, 20.6, 20.6; ESI *m/z* [M+H]$^+$ calculated for C$_{84}$H$_{139}$N$_{10}$O$_{34}$ 1831.95, found 1831.95.

4.2.2.3. Compound 4c. From 95 mg (0.11 mmol) of NHS ester and 200 mg (0.45 mmol) of 6-aminohexyl 2,3,4,6-tetra-O-acetyl-α-D-mannopyranoside (**3c**) there were obtained 90 mg (45%) of compound **4c** as white solid: ^{1}H NMR (CDCl$_3$, 400 MHz): δ 6.64 (br s, 3H, 3 × NH), 6.38 (br s, 1H, NH), 5.31–5.18 (m, 9H, 3 × H-2, 3 × H-3, 3 × H-4), 4.77 (br s, 3H, 3 × H-1), 4.26 (dd, 3H, J = 12.2, 5.3 Hz, 3 × H-6′), 4.08 (dd, 3H, J = 12.2, 2.1 Hz, 3 × H-6), 3.96–3.93 (m, 3H, 3 × H-5), 3.69–3.63 (m, 15H, 3 × OCH'$\underline{H}$", 3 × CC$\underline{H}_2$OC$\underline{H}_2$), 3.41 (dt, 3H, J = 9.5, 6.4 Hz, 3 × OC$\underline{H}$'H"), 3.24–3.20 (m, 8H, 3 × (CH$_2$)$_4$C$\underline{H}_2$NH, N$_3$C$\underline{H}_2$), 2.42 (t, 6H, J = 5.4 Hz, 3 × OCH$_2$C$\underline{H}_2$C(O)), 2.19–2.13 (m, 2H, (CH$_2$)$_8$C$\underline{H}_2$C(O)), 2.13, 2.08, 2.02, 1.97 (all s, 9H each, 12 × C(O)C$\underline{H}_3$), 1.58–1.51 (m, 16H, Aliphatics), 1.37–1.22 (m, 24H, Aliphatics); ^{13}C NMR (CDCl$_3$, 100 MHz): δ 171.8, 170.6, 170.1, 170.0, 169.7, 97.5, 69.6, 69.6, 69.2, 68.4, 68.3, 67.3, 66.1, 62.4, 59.6, 51.4, 39.8, 37.0, 36.1, 29.4, 29.3, 29.2, 29.1, 28.8, 26.7, 26.7, 25.9, 25.8, 20.9, 20.7, 20.7; HRMS *m/z* [M+2H]$^{2+}$ calculated for C$_{84}$H$_{137}$N$_7$O$_{37}$ 917.9521, found 917.9502.

4.2.3. Synthesis of compounds 1b and 1c
4.2.3.1. General procedure. Corresponding compound **4b** or **4c** was dissolved in MeOH and 0.02 M sollution of MeONa in MeOH was added. The reaction mixture was stirred at room temperature for 2 h. Dowex 50W-X8 hydrogen form was added to obtain pH 6. Ion-exchange resin was filtered off and washed with MeOH. The solvent was removed under reduced pressure.

4.2.3.2. Compound 1b. From 50 mg of compound **4b**, 4.5 ml of MeOH and 0.8 ml of MeONa solution there were obtained 30 mg (76%) of compound **1b** as white solid: ^{1}H NMR (D$_2$O, 400 MHz): δ 4.44 (d, J = 8.4 Hz, 3H, 3 × H-1), 3.87–3.80 (m, 6H, 3 × H-2, 3 × H-5), 3.71–3.59 (m, 18H, 3 × H-4, 3 × OC$\underline{H}$'H'', 3 × CC$\underline{H_2}$OC$\underline{H_2}$), 3.54 (m, 6H, 3 × H-3, 3 × OCH'$\underline{H}$''), 3.41–3.37 (m, 6H, 3 × H-6, 3 × H-6′), 3.26 (t, J = 6.8 Hz, 2H, N$_3$C$\underline{H_2}$), 3.13 (t, J = 6.9 Hz, 6H, 3 × (CH$_2$)$_4$C$\underline{H_2}$NH), 2.41 (t, J = 5.6 Hz, 6H, 3 × OCH$_2$C$\underline{H_2}$C(O)), 2.16 (t, J = 7.0 Hz, 2H, (CH$_2$)$_8$C$\underline{H_2}$C(O)), 1.97 (s, 9H, 3 × NHAc), 1.57–1.45 (m, 16H, Aliphatics), 1.32–1.22 (m, 24H, Aliphatics); ^{13}C NMR (D$_2$O, MHz): δ 174.2, 174.1, 173.6, 101.1, 75.8, 73.8, 70.2, 69.9, 67.5, 60.7, 59.9, 55.6, 51.2, 39.4, 36.5, 36.2, 28.9, 28.7, 28.6, 28.6, 28.4, 28.2, 26.2, 25.9, 25.4, 24.9, 22.2; HRMS *m/z* [M + 2K]$^{2+}$ calculated for C$_{66}$H$_{120}$N$_{10}$O$_{25}$K$_2$ 765.3845, found 765.3821.

4.2.3.3. Compound 1c. From 50 mg of compound **4c**, 4.5 ml of MeOH and 0.8 ml of MeONa solution there were obtained 32 mg (78%) of compound **1c** as white solid; ^{1}H NMR (D$_2$O, 400 MHz): δ 4.80 (br s, 3H, 3 × H-1), 3.87 (br s, 3H, 3 × H-5), 3.88–3.80 (m, 3H, 3 × H-2), 3.76–3.53 (m, 27H, 3 × H-4, 3 × CC$\underline{H_2}$OC$\underline{H_2}$, 3 × H-3, 3 × CH$_2$-6, 3 × OCH'$\underline{H}$''), 3.47 (dt, J = 9.6, 6.1 Hz, 3H, 3 × OC$\underline{H}$'H''), 3.26 (t, J = 6.7 Hz, 2H, N$_3$C$\underline{H_2}$), 3.15 (t, J = 6.5 Hz, 6H, 3 × (CH$_2$)$_4$C$\underline{H_2}$NH), 2.43 (br s, 6H, 3 × OCH$_2$C$\underline{H_2}$C(O)), 2.18 (br s, 2H, (CH$_2$)$_8$C$\underline{H_2}$C(O)), 1.56–1.44 (m, 16H, Aliphatics), 1.33–1.27 (m, 24H, Aliphatics); ^{13}C NMR (D$_2$O, 100 MHz): δ 173.3, 99.7, 72.7, 70.7, 70.2, 68.9, 67.6, 66.6, 60.8, 51.2, 39.3, 36.4, 36.2, 28.9, 28.9, 28.8, 28.7, 28.6, 28.5, 26.2, 26.1, 25.3. ESI *m/z* [M + H]$^{+}$ calculated for C$_{60}$H$_{112}$N$_7$O$_{25}$ 1330.77, found 1330.70; ESI *m/z* [M + HCOO]$^{-}$ calculated for C$_{61}$H$_{112}$N$_7$O$_{27}$ 1374.76, found 1374.76.

4.2.4. Synthesis of conjugates 5a-5c

4.2.4.1. General procedure. To the appropriate ligand **1a**, **1b** or **1c** (12 mg, 8 μmole) dissolved in water (2.5 mL) was added *sulfo*-Cy5 alkyne (5 mg, 7 μmole) in dry DMF (2.5 mL). The mixture was degassed and filled with argon. 0.05 M solution of sodium ascorbate (160 μl) and 0.05 M solution of copper iodide (140 μl) were added and the mixture was stirred at room temperature for 12 h. After that, 0.05 M solution of disodium EDTA (140 μl) was added and the mixture was concentrated under reduced pressure. The residue was dissolved in ethanol and cooled to 0°C. Precipitate was filtered off and filtrate was concentrated under reduced pressure. Compounds **5b** and **5c** were additionally purified by HPLC.

4.2.4.2. Compound 5a. Yield 14 mg (94%), blue solid: Electronic absorption spectrum: λ_{max} = 646 nm; ^{1}H NMR (D$_2$O, 400 MHz): δ 8.04 (br s, 2H, –CH=), 7.82–7.78 (m, 4H, ArH, ArH$_{TRZ}$), 7.31 (d, J = 7.8 Hz, 1H, ArH), 7.24 (d, J = 7.7 Hz, 1H, ArH), 6.53 (t, J = 11.3 Hz, 1H, =CH-), 6.21 (d, J = 13.3 Hz, 1H, =CH-), 6.15 (d, J = 11.4 Hz, 1H, = CH-), 4.39 (d, J = 8.2 Hz, 1H, H-1), 4.29 (br s, 2H, N$^+$C$\underline{H_2}$), 3.95–3.56 (m, 40H, 3 × H-2, 3 × H-3, 3 × H-4, 3 × H-5, 6 × H-6, 3 × OC$\underline{H}$'H'', C$\underline{H_2}$(CH$_2$)$_9$, 3 × CC$\underline{H_2}$OC$\underline{H_2}$, CH$_3$N, C$\underline{H_2}$-TRZ), 3.50–3.46 (m, 3H, 3 × OCH'$\underline{H}$''), 3.09 (t, J = 6.6 Hz, 6H, 3 × NHC$\underline{H_2}$(CH$_2$)$_5$OGalNAc), 2.41–2.39 (m, 6H, 3 × OCH$_2$C$\underline{H_2}$CO), 2.21 (br s, 2H, N$_3$CH$_2$(CH$_2$)$_8$C$\underline{H_2}$CONH), 2.08 (t, J = 6.4 Hz, 2H, C$\underline{H_2}$CONH), 1.98 (s, 9H, 3 × C$\underline{H_3}$CONH), 1.72–1.23 (m, 48H, Aliphatics), 1.05–1.01 (m, 10H, Aliphatics); HRMS *m/z* [M-H]$^{2-}$ calculated for C$_{101}$H$_{159}$N$_{13}$O$_{32}$S$_2$ 1065.0333, found 1065.0330.

4.2.4.3. Compound 5b. Yield 13 mg (87%), blue solid: Electronic absorption spectrum: λ_{max} = 646 nm; ^{1}H NMR (D$_2$O, MHz): δ 8.01–7.96 (m, 2H, =CH-), 7.81–7.73 (m, 5H, ArH, ArH$_{TRZ}$), 7.25 (d, J = 8.1 Hz, 1H, ArH), 7.19 (d, J = 8.0 Hz, 1H, ArH), 6.45 (t, J = 11.1 Hz, 1H, =CH-), 6.16–6.06 (m, 2H, =CH-), 4.40 (d, J = 8.4 Hz, 3H, 3 × H-1), 4.35–4.20 (m, 4H, N$^+$C$\underline{H_2}$, NH), 3.84–3.34 (m, 43H, 3 × H-2, 3 × H-3, 3 × H-4, 3 × H-5, 6 × H-6, 3 × OC$\underline{H}$'H'', C$\underline{H_2}$(CH$_2$)$_9$, 3 × CC$\underline{H_2}$OC$\underline{H_2}$, CH$_3$N, C$\underline{H_2}$-TRZ), 3.04 (t,

J = 6.1 Hz, 6H, 3 × NHC$\underline{H_2}$(CH$_2$)$_5$OGlcNAc), 2.39–2.35 (m, 6H, 3 × OCH$_2$C$\underline{H_2}$CO), 2.18–2.15 (m, 2H, (CH$_2$)$_8$C$\underline{H_2}$CONH), 2.02 (t, J = 5.5 Hz, 2H, C$\underline{H_2}$CONH), 1.94 (s, 9H, 3 × C$\underline{H_3}$CONH), 1.70–1.17 (m, 48H, Aliphatics), 1.05–0.94 (m, 10H, Aliphatics); HRMS *m/z* [M-H]$^{2-}$ calculated for C$_{101}$H$_{159}$N$_{13}$O$_{32}$S$_2$ 1065.0333, found 1065.0326.

4.2.4.4. Compound 5c. Yield 9 mg (60%), blue solid: Electronic absorption spectrum: λ_{max} = 646 nm; ^{1}H NMR (D$_2$O, MHz): δ 8.06–7.99 (m, 2H, =CH-), 7.79–7.73 (m, 5H, ArH, ArH$_{TRZ}$), 7.28 (d, J = 8.5 Hz, 1H, ArH), 7.20 (d, J = 9.2 Hz, 1H, ArH), 6.45 (t, J = 12.5 Hz, 1H, =CH-), 6.14 (d, J = 13.3 Hz, 1H, =CH-), 6.08 (d, J = 11.2 Hz, 1H, =CH-), 4.33 (br s, 3H, 3 × H-1), 4.29–4.26 (m, 2H, N$^+$C$\underline{H_2}$), 3.95–3.34 (m, 43H, 3 × H-2, 3 × H-3, 3 × H-4, 3 × H-5, 6 × H-6, 3 × OC$\underline{H}$'H'', C$\underline{H_2}$(CH$_2$)$_9$, 3 × CC$\underline{H_2}$OC$\underline{H_2}$, CH$_3$N, C$\underline{H_2}$-TRZ), 3.04 (t, J = 7.0 Hz, 6H, 3 × NHC$\underline{H_2}$(CH$_2$)$_5$O), 2.34 (t, J = 5.5 Hz, 6H, 3 × OCH$_2$C$\underline{H_2}$CO), 2.18 (t, J = 6.7 Hz, 2H, (CH$_2$)$_8$C$\underline{H_2}$CONH), 2.03 (t, J = 7.3 Hz, 2H, C$\underline{H_2}$CONH), 1.72–1.20 (m, 48H, Aliphatics), 1.01–0.98 (m, 10H, Aliphatics); HRMS *m/z* [M + 3Na]$^{2+}$ calculated for C$_{95}$H$_{151}$N$_{10}$O$_{32}$S$_2$Na$_3$, 1038.4810, found 1038.4828.

4.3. Liver intravital imaging

BALB/c female mice were anesthetized by i.p. injection of 200 mg/kg ketamine with 5 mg/kg xylazine. Tail vein was cannulated and fluorescently labeled antibodies (4 μL Ly6G BV-421, 7 μL F4/80 Alexa-488, Biolegend) were injected to stain host cells *in vivo*. Liver preparations were made by making a midline incision followed by a lateral incision along the costal margin to the midaxillary line, which was performed to expose the liver. The mouse was placed in a right lateral position, and the ligaments attaching the liver to the diaphragm and the stomach were cut, allowing the liver to be externalized onto a glass coverslip on the heated stage of inverted confocal microscope Nikon A1R. Exposed abdominal tissues were covered with saline-soaked gauze to prevent dehydration. The liver was draped with a saline soaked tissue to avoid tissue dehydration and to help restrict movement of the tissue on the slide. IVM was performed using a Plan Apo 20x/0,75 DIC N objective and Apo LWD 40x/1,15 S water immersion objective. Images were scanned sequentially using 405-, 488-and 647-nm diode lasers in combination with a DM405/488/561/633-nm dichroic beam splitter. Five to ten spots were imaged at the time and within 2 h after i.v. injection of 200 μL fluorescently tagged conjugates (3 mg/kg Cy5; n = 3 for each group) with acquisition rate 2–3 frames/min. Imaging analysis was performed using NIS Elements AR software.

Declaration of competing interest

The authors declare that they have no known competing financial interests or personal relationships that could have appeared to influence the work reported in this paper.

Appendix A. Supplementary data

Supplementary data to this article can be found online at https://doi.org/10.1016/j.carres.2020.107928.

References

[1] P.V. Devarajan, S. Jain (Eds.), Targeted Drug Delivery: Concepts and Design, Springer, New York, 2015.

[2] A.D. Springer, S.F. Dowdy, GalNAc-siRNA conjugates: leading the way for delivery of RNAi therapeutics, Nucleic Acid Therapeut. 28 (2018) 109–118, https://doi.org/10.1089/nat.2018.0736.

[3] Y.A. Ivanenkov, S.Yu Maklakova, E.K. Beloglazkina, N.V. Zyk, A.G. Nazarenko, A.G. Tonevitsky, V.E. Kotelianski, A.G. Majouga, Development of liver cell-targeted drug delivery systems: experimental approaches, Russ. Chem. Rev. 86 (2017) 750–776, https://doi.org/10.1070/RCR4707.

[4] A.A. D'Souza, P.V. Devarajan, Asialoglycoprotein receptor mediated hepatocyte targeting—strategies and applications, J. Contr. Release 203 (2015) 126–139, https://doi.org/10.1016/j.jconrel.2015.02.022.

[5] X. Huang, J.C. Leroux, B. Castagner, Well-defined multivalent ligands for hepatocytes targeting via asialoglycoprotein receptor, Bioconjugate Chem. 28 (2016) 283–295, https://doi.org/10.1021/acs.bioconjchem.6b00651.

[6] T.P. Prakash, J. Yu, M.T. Migawa, G.A. Kinberger, W.B. Wan, M.E. Østergaard, R.L. Carty, G. Vasquez, A. Low, A. Chappell, K. Schmidt, M. Aghajan, J. Crosby, H.M. Murray, S.L. Booten, J. Hsiao, A. Soriano, T. Machemer, P. Cauntay, S.A. Burel, S.F. Murray, H. Gaus, M.J. Graham, E.E. Swayze, P.P. Seth, Comprehensive structure–activity relationship of triantennary N-acetylgalactosamine conjugated antisense oligonucleotides for targeted delivery to hepatocytes, J. Med. Chem. 59 (2016) 2718–2733, https://doi.org/10.1021/acs.jmedchem.5b01948.

[7] R.A. Petrov, S.Yu Maklakova, YaA. Ivanenkov, S.A. Petrov, O.V. Sergeeva, E.Yu Yamansarov, I.V. Saltykova, I.I. Kireev, I.B. Alieva, E.V. Deyneka, A.A. Sofronova, A.V. Aladinskaia, A.V. Trofimenko, R.S. Yamidanov, S.V. Kovalev, V.E. Kotelianski, T.S. Zatsepin, E.K. Beloglazkina, A.G. Majouga, Synthesis and biological evaluation of novel mono- and bivalent ASGP-R-targeted drug-conjugates, Bioorg. Med. Chem. Lett 28 (2018) 382–387, https://doi.org/10.1016/j.bmcl.2017.12.032.

[8] S.Yu Maklakova, F.A. Kucherov, R.A. Petrov, V.V. Gopko, G.A. Shipulin, T.S. Zatsepin, E.K. Beloglazkina, N.V. Zyk, A.G. Majouga, V.E. Kotelianski, A new approach to the synthesis of ligands of asialoglycoprotein receptor for targeted delivery of oligonucleotides to hepatocytes, Russ. Chem. Bull. 64 (2015) 1655–1662, https://doi.org/10.1007/s11172-015-1056-6.

[9] K.-L. Hou, P.-Y. Chiang, C.-H. Lin, B.-Y. Li, W.-T. Chien, Y.-T. Huang, C.-C. Yu, C.-C. Lin, Water-soluble sulfo-fluorous affinity (SOFA) tag-assisted enzymatic synthesis of oligosaccharides, Adv. Synth. Catal. 360 (2018) 2313–2323, https://doi.org/10.1002/adsc.201800085.

[10] M. Gade, C. Alex, S.L. Ben-Arye, J.T. Monteiro, S. Yehuda, B. Lepenies, V. Padler-Karavani, R. Kikkeri, Microarray analysis of oligosaccharide-mediated multivalent carbohydrate–protein interactions and their heterogeneity, Chembiochem 19 (2018) 1170–1177, https://doi.org/10.1002/cbic.201800037.

[11] V. Shmendel, A.A. Timakova, M.A. Maslov, N.G. Morozova, V.V. Chupin, Synthesis of mannose-containing neoglycolipids as a component of targeted delivery system for transfer of nucleic acids into antigen-presenting cells, Russ. Chem. Bull. 61 (2012) 1497–1501, https://doi.org/10.1007/s11172-012-0194-3.

[12] J.H. Kang, R. Toita, M. Murata, Liver cell-targeted delivery of therapeutic molecules, Crit. Rev. Biotechnol. 36 (2016) 132–143, https://doi.org/10.3109/07388551.2014.930017.

[13] J.J. Reina, A. Rioboo, J. Montenegro, Glycosyl aldehydes: new scaffolds for the synthesis of neoglycoconjugates via bioorthogonal oxime bond formation, Synthesis 50 (2018) 831–845, https://doi.org/10.1055/s-0036-1591082.

[14] M. Mori, Y. Ito, T. Ogawa, Total synthesis of the mollu-series glycosyl ceramides α-d-Manp-(1→3)-β-d-Manp-(1→4)-β-d-Glcp-(1→1)-Cer and α-d-Manp-(1→3)-[β-d-Xylp-(1→2)]-β-d-Manp-(1→4)-β-d-Glcp-(1→1)-Cer, Carbohydr. Res. 195 (1990) 199–224, https://doi.org/10.1016/0008-6215(90)84167-S.